Electrical properties of Nb–$MoSi_2$–Nb Josephson junctions

Yonuk Chong,[a] P. D. Dresselhaus, and S. P. Benz
National Institute of Standards and Technology, Boulder, Colorado 80305

(Received 31 January 2005; accepted 6 May 2005; published online 3 June 2005)

We present a detailed study of the electrical properties of planar Nb–$MoSi_2$–Nb Josephson junctions. The Nb–$MoSi_2$–Nb junction is an excellent system to study proximity coupling in junctions with rigid superconductor/normal metal boundaries by precisely and independently controlling the barrier thickness and the temperature. With regard to applications, the Josephson properties are very reproducible, and the characteristic voltage can be tuned easily over more than two orders of magnitude while still maintaining a practical critical current density. The characteristic voltage can be controlled within ±5% at 4 K, with an exponential dependence on the barrier thickness. The proximity-coupled junction theory fits the temperature dependence of the critical current density, allowing us to quantitatively extract material parameters. [DOI: 10.1063/1.1947386]

Non-hysteretic superconductor-normal metal-superconductor (SNS) Josephson junctions, in which two superconductors are coupled by the proximity effect through a normal metal barrier, have been considered for many superconducting electronics applications.[1–4] These overdamped junctions have a variety of current and prospective applications such as fast-programmable voltage standards, rapid single flux quantum digital circuits, and dc superconducting quantum interference devices. However, these applications will be realized only if SNS junctions can be made with reproducible and uniform electrical characteristics, such as the Josephson critical current density J_c and the characteristic voltage V_c (defined as the product of the critical current I_c and the normal resistance R_n). We demonstrate in this letter an SNS junction technology that meets these challenging criteria.

One of the most important electrical parameters for applications is V_c, because it determines the junction characteristic frequency $2eV_c/h$ and the effective switching speed of the junction. Because high current density typically accompanies high characteristic voltages, it is difficult to achieve practical (<10 mA) critical currents with micrometer-scale fabrication processes. Thus, the primary challenge in making useful SNS junctions is to maintain a high characteristic voltage while reducing the critical current density. For example, planar, sandwich-type SNS junctions cannot use high-conductivity metal barriers, such as Cu or Au, because they have extremely high critical current density. In order to achieve practical critical currents in those junctions, V_c cannot be increased too much unless we fabricate nanoscale junctions that would suffer from nonuniformity. Low V_c in SNS junctions can also be caused by a reduction of the order parameter at the superconductor/normal metal (S/N) interface. This reduction, called a "soft boundary condition", is caused by the interdiffusion of quasiparticles from the superconductor with the electrons from the normal metal. Hence, highly conducting-metal barrier junctions have a maximal V_c that is far lower than the energy gap voltage of the superconducting electrodes.[3] In addition, the interface resistance at the low-transparency S/N boundary can also cause a reduction in V_c.

At the National Institute of Standards and Technology (NIST), we achieved higher V_c for Josephson voltage standard applications by choosing high-resistivity alloys as barrier materials. For many years, we focused on PdAu as a useful barrier material,[4] but for practical current densities the maximal V_c was still limited to about 50 μV. More recently, we found that $MoSi_2$ barriers can overcome the two major obstacles of extremely high critical current density and reduced V_c from soft S/N boundaries. Because $MoSi_2$ has high resistivity ($\rho_N \sim 750\ \mu\Omega$ cm at 4 K), we can make high-V_c junctions ($V_c = J_c \rho_N d$) with lower critical current density than that of junctions with more conductive barriers. Furthermore, the mismatch in the electronic properties between $MoSi_2$ and Nb makes the S/N boundary "rigid"; that is, there is no noticeable suppression of the order parameter at the S/N interface.[5] The measured boundary resistance R_B between these two materials is very small, which is an indication that the interface has good transparency.[5,6] These factors enable a highly controllable and reproducible junction fabrication process, and make the Nb–$MoSi_2$–Nb junction an excellent system in which to study the proximity effect without any unknown physical variables. Also, this is the first system with rigid S/N interfaces that can be modeled theoretically with good control in fabrication.

One particular merit of the $MoSi_2$-barrier junctions is that they can be tuned over a wide range of characteristic voltages while still maintaining practical critical current density. These junctions have already been successfully applied to high-performance programmable Josephson voltage standards in the form of stacked junctions with over 100 000 junctions simultaneously operating with uniform electrical characteristics.[7,8].

The barrier material is an amorphous $MoSi_2$ film that is dc sputter deposited at ambient substrate temperature from a sintered stoichiometric target. The resistivity shows nearly flat temperature dependence from 300 K to 4 K, and no superconducting transition has been observed down to 50 mK. Details of the junction fabrication process were reported elsewhere.[9] In this letter, we report a detailed study of the electrical properties of $MoSi_2$-barrier Josephson junctions and quantitatively extract relevant material parameters.

We assume that the barrier thickness d is much larger than the normal metal coherence length $\xi_N(T)$. We adopt the conventional dirty-limit theory of the proximity-coupled junctions[3,10] to understand the behavior of our junctions.

[a]Present address: Korea Research Institute of Standards and Science, Daejeon 305–600, Korea; electronic mail: yonuk@kriss.re.kr

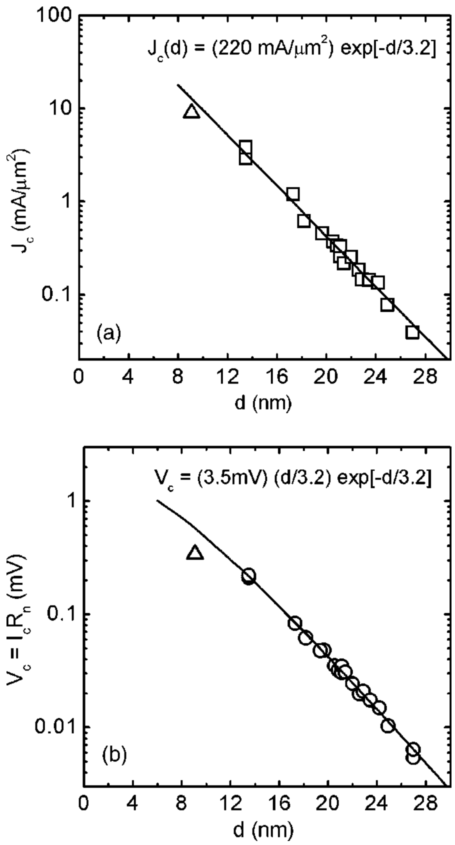

FIG. 1. Data of (a) J_c and (b) V_c at 4 K as a function of the $MoSi_2$ barrier thickness d. The lines are fit to Eqs. (3) and (4).

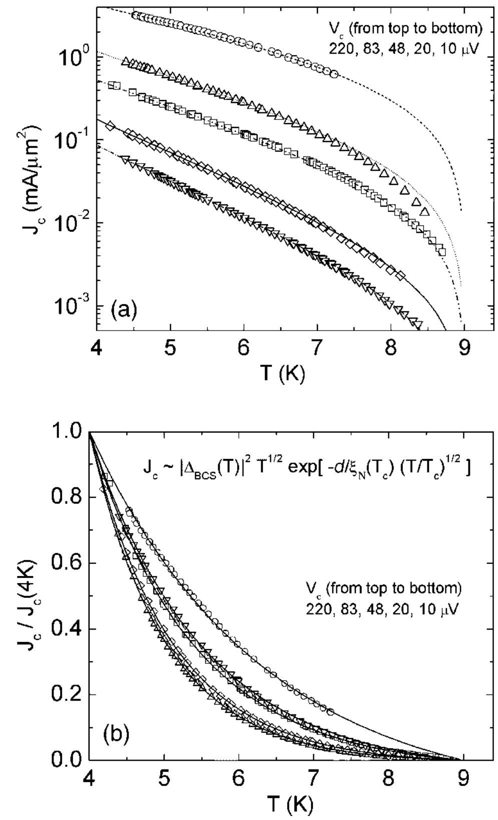

FIG. 2. (a) Temperature dependence of J_c in junctions with different barrier thicknesses. (b) The same data with a linear current density scale, normalized to J_c(4 K). Symbols are the measured data, and the lines are fit using Eq. (1) with the fitting parameters given in Table I.

When a normal metal is sandwiched between two superconductors, J_c depends on two variables, the normal metal thickness d and the temperature T, as

$$J_c(d,T) = \left(\frac{\pi}{2e\rho_N \xi_N(T)} \frac{|\Delta_i(T)|^2}{k_B T_c}\right) \exp[-d/\xi_N(T)] \quad d \gg \xi_N(T)$$
$$\propto |\Delta_i(T)|^2 \cdot T^{1/2} \exp[-d/\xi_N(T_c)(T/T_c)^{1/2}], \tag{1}$$

where

$$\xi_N(T) = \left(\frac{\hbar D_N}{2\pi k_B T}\right)^{1/2} \quad \text{when } \xi_N \gg l_N \text{ (dirty limit)}. \tag{2}$$

These equations are valid in the temperature range $0.3T_c < T < T_c$, where T_c is the critical temperature of the superconductor. The more elaborate microscopic theory[11] gives only minor corrections to the prefactor of Eq. (1). Here ρ_N is the normal metal resistivity, $\Delta_i(T)$ is the order parameter at the S/N interface, and $D_N = v_F \ell_N / 3$ is the diffusion constant with the Fermi velocity v_F and the mean-free path ℓ_N of the normal metal barrier. Both the superconductor (Nb) and the barrier ($MoSi_2$) are assumed to be in the dirty limit, $\xi_{N,S}(\text{clean}) \gg \ell_{N,S}$. At a fixed temperature, Eq. (1) can be simplified as

$$J_c(d) = J_{c0} e^{-d/\xi_N}, \tag{3}$$

$$V_c(d) = I_c R_n(d) = V_{c0}(d/\xi_N) e^{-d/\xi_N}, \tag{4}$$

where J_{c0} and V_{c0} are constants.

Figure 1 shows the critical current density J_c and the characteristic voltage V_c at 4 K as a function of the $MoSi_2$ barrier thickness d. These data are from a series of samples made over a period of more than a year, with two different $MoSi_2$ sputter targets. The $MoSi_2$ barrier thicknesses are nominal values calculated from the deposition time and the calibrated rate. By fitting the data to Eqs. (3) and (4) we determined the fitting parameters $J_{c0} = 220\ mA/\mu m^2$ and $V_{c0} = 3.5$ mV with the same normal coherence length at 4 K of $\xi_N = 3.2$ nm.[12] The data (triangle) for the highest current density, 9 nm barrier do not fit to the theory because the junctions are no longer in the small-junction limit and are beginning to exhibit current crowding due to large-junction behavior.[13] The prefactors are in good agreement (within ~30%) with the theory using the measured material parameters and the 1.5 meV energy gap of Nb from the literature.[14]

Figure 2 shows the temperature dependence of the critical current density for different barrier thicknesses. The data fit well with Eq. (1) using $\xi_N(T_c)$ and $\Delta_i(T=0)$ as fitting parameters, and T_c is chosen to be 9 K for the best overall fit. We assumed the BCS energy gap for the temperature dependence of $\Delta_i(T)$. The resulting values of the fitting parameters are given in Table I. The normal coherence length at T_c, $\xi_N(T_c)$, can also be independently calculated by use of Eq. (2) and the value of $\xi_N(4\text{ K})$ that was obtained from the thickness dependence of J_c and V_c [Figs. 1(a) and 1(b)], which gives $\xi_N(T_c) = 2.1$ nm. We compare this value with $\xi_N(T_c) = 1.9$ nm in Table I, which was obtained from the temperature dependence; they agree within ~10%. Also the gap values $\Delta_i(T=0)$ in Table I are close to the nominal Nb gap value, but tend to be slightly overestimated. However, the accuracy of this estimation may depend on the details of the model and the prefactor of Eq. (1) as well as the accuracy of

TABLE I. Fitting parameter values from the measured temperature dependence of the current density J_c. Barrier thickness d is given by the nominal value from the deposition time and a fixed rate of 17.6 nm/min. The characteristic voltage V_c is measured from the $I-V$ curves. The fitting parameters are normal metal coherence length $\xi_N(T_c)$, the superconducting energy gap at the S/N interface $\Delta_i(T=0)$. The Nb superconducting transition temperature T_c was chosen to be 9.0 K that yielded the best overall fit.

d (nm)	$V_c(\mu V)$	$\xi_N(T_c)$ (nm)	$\Delta_i(T=0)$ (meV)	T_c (K)
13.5	220	2.00	2.1	9.0
17.3	83	1.88	2.7	9.0
19.4	48	1.98	2.0	9.0
22.6	20	1.87	2.5	9.0
24.9	10	1.91	2.4	9.0

the measurement. Given $\xi_N(T_c) \sim 2$ nm, using Eq. (2) we estimate the diffusion constant of $MoSi_2$ at T_c (and also at 4 K) to be $D_N \sim 3 \times 10^{-5}$ m^2/s. Quantitatively knowing these material parameters, we can now accurately predict and design $MoSi_2$-barrier junctions over a large range of electrical characteristics.

Another test for the proximity junction theory is to study the asymptotic behavior of $J_c(T)$ near T_c and look at the exponent α of $J_c \propto (T-T_c)^\alpha$. A perfectly soft S/N boundary will be described with α of 2, and the perfectly rigid S/N boundary (as in the tunnel junction) would have α of 1.[3] The estimate of this exponent, however, depends strongly on the choice of T_c as well as the accuracy of the measurement of I_c near T_c. When we chose data points within 10% of T_c, we found that the exponent α varies between 1.1 to 1.5, depending on the samples and the choice of T_c. In any case, a value of the exponent near unity indirectly implies that our S/N boundary is in the rigid regime, which is also consistent with the fact that fitting parameters $\Delta_i(T=0)$ in Table I are close to the energy gap of Nb. We can also confirm that these $MoSi_2$-barrier junctions are in the rigid regime from our estimation of the suppression parameters,[15] $\gamma = \rho_S \xi_S / \rho_N \xi_N = 0.03$ and $\gamma_B = R_B / \rho_N \xi_N < 0.8$, where $\rho_S(10\text{ K}) = 4\ \mu\Omega$ cm and $\xi_S(4\text{ K}) = 17.5$ nm are the normal resistivity and the coherence length of Nb.[5,6]

Figure 3 shows the normalized current-voltage (I-V) curves at 4 K for barriers with different V_c. We note that the shape of the I-V characteristic changes for different barrier thicknesses. As the barrier gets thinner, or as the V_c and J_c get larger, the transition from the zero voltage state to the voltage state at I_c becomes sharper, and eventually the junction becomes nearly hysteretic. Comparing the I-V characteristics with the resistively shunted junction (RSJ) model without capacitance, we can say empirically that the I-V curve for $V_c = 48\ \mu$V most closely matches the curvature of the RSJ model. This also corresponds to a barrier thickness of ~20 nm [or $d/\xi_N(4\text{ K}) \sim 6.2$]. When V_c is greater than 50 μV or the barrier is thinner than 20 nm, the measured transitions to the voltage state become increasingly sharper than that expected for the RSJ model, while junctions with barriers thicker than 20 nm show transitions to the voltage state that become increasingly less sharp than that of the RSJ model. Further study would be required to understand these shape changes.

In conclusion, we present a quantitative analysis of electrical properties of $MoSi_2$-barrier SNS Josephson junctions with independent and precise control of the barrier thickness and operating temperature. Our comprehensive measurements and detailed results on Nb–$MoSi_2$–Nb junctions confirm that they provide both an excellent model system to study the theory of proximity effect and good candidates for large-scale integrated Josephson circuits. This is the first study of rigid-boundary SNS junctions with characteristics that are sufficiently uniform, reproducible, and appropriate for practical applications.

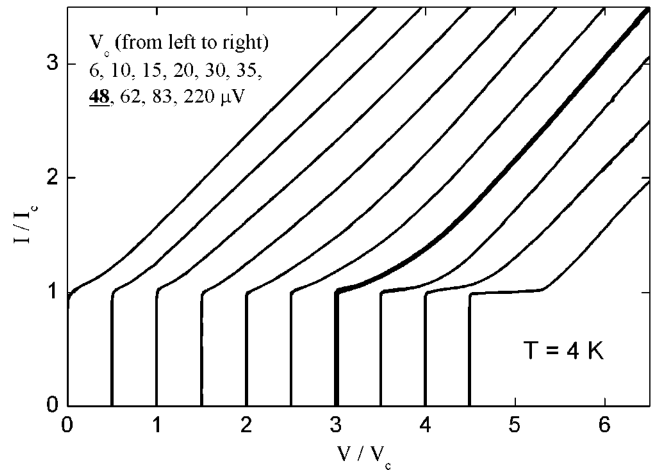

FIG. 3. Normalized junction I-V characteristics measured at 4 K with different barrier thicknesses, or equivalently different V_c and J_c. The V_c's are 6, 10, 15, 20, 30, 35, 48, 62, 83, and 220 μV from left to right. The curves are measured in square geometry junctions with 3.5 to 4.5 μm width, except for the two highest V_c junctions in which we used smaller junctions with size of 2.5 μm and 0.4 μm, respectively. The highest V_c junction (220 μV) is nearly hysteretic showing a rapid transition to the voltage state at I_c. The curves are shifted in the voltage axis for clarity.

The authors thank Nicolas Hadacek for valuable discussions. This work was supported in part by the office of Naval Research Contract Nos. N0001404IP20044 and N0001405IP20017.

[1] P. G. de Gennes, *Superconductivity of Metals and Alloys* (W. A. Benjamin, New York, 1966).
[2] J. Clarke, Proc. R. Soc. London, Ser. A **308**, 447 (1969).
[3] K. A. Delin and A. W. Kleinsasser, Supercond. Sci. Technol. **9**, 227 (1996).
[4] S. P. Benz, Appl. Phys. Lett. **67**, 2714 (1995).
[5] Y. Chong, P. D. Dresselhaus, S. P. Benz, and J. E. Bonevich, Appl. Phys. Lett. **82**, 2467 (2003).
[6] The interface resistance times the area, R_B, was extrapolated from the junction resistance R_n times the junction area vs the barrier thickness d plot. This only gives the upper limit of the contribution from the interface. R_B is estimated to be $<10^{-10}\ \Omega$ cm^2.
[7] Y. Chong, C. J. Burroughs, P. D. Dresselhaus, N. Hadacek, H. Yamamori, and S. P. Benz, IEEE Trans. Instrum. Meas. **54**, 616 (2005).
[8] Y. Chong, C. J. Burroughs, P. D. Dresselhaus, N. Hadacek, H. Yamamori, and S. P. Benz, IEEE Trans. Appl. Supercond. (to be published).
[9] P. D. Dresselhaus, Y. Chong, J. H. Plantenberg, and S. P. Benz, IEEE Trans. Appl. Supercond. **13**, 930 (2003).
[10] P. G. de Gennes, Rev. Mod. Phys. **36**, 225 (1964).
[11] K. K. Likharev, Rev. Mod. Phys. **51**, 101 (1979).
[12] This value differs from the previous estimation [Chong *et al.*, Appl. Phys. Lett. **82**, 2467 (2003)] by ~10% because we have carefully recalibrated the barrier deposition rate to be 17.6 nm/min instead of 19.7 nm/min used before. This does not qualitatively affect any of the previous results, but the thickness scales of $MoSi_2$ in Chong *et al.* should be multiplied by 0.9.
[13] R. L. Kautz, J. Appl. Phys. **78**, 5811 (1995).
[14] T. P. Orlando and K. A. Delin, *Foundations of Applied Superconductivity* (Addison–Wesley, Reading, MA, 1991).
[15] M. Y. Kupriyanov and V. F. Lukichev, Sov. Phys. JETP **67**, 1163 (1988).